On the Time-Development of Sulphate Hydration in Anhydritic Swelling Rocks

Rock Mech Rock Eng (2013) 46:619–634
DOI 10.1007/s00603-013-0376-9

ORIGINAL PAPER

On the Time-Development of Sulphate Hydration in Anhydritic Swelling Rocks

K. Serafeimidis · G. Anagnostou

Received: 3 January 2013 / Accepted: 14 January 2013 / Published online: 2 February 2013

Abstract Anhydritic claystones are among the most problematic rocks in tunnelling. Their swelling has caused serious damage and high repair costs in a number of tunnels, especially in Switzerland and southwest Germany. The swelling is usually attributed to the transformation of anhydrite into gypsum. It is a markedly time-dependent process which might take several decades to complete in nature. The present paper focusses on simultaneous anhydrite dissolution and gypsum precipitation in a closed system, i.e. disregarding the transport processes that may also be important for the evolution of the swelling process. The paper begins with a presentation of the governing equations and continues with parametric studies in order to investigate the role of the initial volumetric fractions of the constituents and the specific surface areas of the minerals involved. A simplified model for the hydration of anhydrite is also proposed, which identifies the governing process and the duration of the swelling process. Finally, parametric studies are performed in order to investigate the effect of the anhydrite surface being sealed by the formation of gypsum. The latter slows down the swelling process considerably.

Keywords Anhydrite · Gypsum · Swelling · Time evolution · Sealing

List of Symbols

A	Mineral surface area in contact with water
A	Shape factor of parellelepipedic particles
a_A	Shape factor of parellelepipedic anhydrite particles
a_G	Shape factor of parellelepipedic gypsum particles
b	Shape factor of parellelepipedic particles
b_A	Shape factor of parellelepipedic anhydrite particles
b_G	Shape factor of parellelepipedic gypsum particles
c	Ion concentration
$\tilde{c}$	Normalized concentration
c_0	Initial concentration
$\tilde{c}_0$	Normalized initial concentration
c_{eq}	Equilibrium concentration
$c_{eq,A}$	Anhydrite equilibrium concentration
$c_{eq,G}$	Gypsum equilibrium concentration
$\tilde{c}_{eq,G}$	Normalized gypsum equilibrium concentration
c_{max}	Maximum concentration
F	Specific surface area
F_A	Anhydrite specific surface area
F_P	Specific surface area of particles consisting of inert solid and gypsum
F_S	Inert solid specific surface area
J	Diffusive flux
K	Reaction rate constant
$\tilde{k}$	Diffusion coefficient
k_A	Reaction rate constant for anhydrite dissolution
k_G	Reaction rate constant for gypsum precipitation
m	Mass per unit volume of the mixture
m_A	Anhydrite mass per unit volume of the mixture
m_{A0}	Initial anhydrite mass per unit volume of the mixture
m_I	Ion mass per unit volume of the mixture
m_{I0}	Initial ion mass per unit volume of the mixture
m_G	Gypsum mass per unit volume of the mixture
m_{G0}	Initial gypsum mass per unit volume of the mixture
m_W	Water mass per unit volume of the mixture
m_{W0}	Initial water mass per unit volume of the mixture
M	Mass

K. Serafeimidis (✉) · G. Anagnostou
ETH Zurich, Switzerland
e-mail: konstantinos.serafeimidis@igt.baug.ethz.ch

n_G Porosity of the gypsum layer
s Distance of the mineral surface from its initial surface
S_0 Characteristic length (thickness and diameter for parellelepipedic and spherical particles, respectively)
s_A Thickness of dissolved anhydrite
$\bar{s}_A$ Normalized thickness of dissolved anhydrite
S_A Characteristic length of anhydrite particles
$\bar{S}_A$ Normalized characteristic length of anhydrite particles
S_{A0} Initial characteristic length of anhydrite particles
s_G Gypsum layer thickness
$\bar{s}_G$ Normalized gypsum layer thickness
S_{G0} Initial characteristic length of gypsum particles
$S_{G,A}$ Characteristic length of gypsum particles for growth on anhydrite
$\bar{S}_{G,A}$ Normalized characteristic length of gypsum particles for growth on anhydrite
$S_{G,G}$ Characteristic length of gypsum particles for growth on gypsum
$\bar{S}_{G,G}$ Normalized characteristic length of gypsum particles for growth on gypsum
$S_{G,S}$ Characteristic length of gypsum particles for growth on inert minerals
$\bar{S}_{G,S}$ Normalized characteristic length of gypsum particles for growth on inert minerals
S_S Inert solid particles diameter
$\bar{S}_S$ Normalized diameter of inert solid particles
T Time
t_d Time at which sealing becomes the relevant mechanism
T_G Gypsum layer tortuosity
V Volume
V_{tot} Total volume of the mixture
$V_{tot,0}$ Initial total volume of the mixture

Greek Symbols

α Order of chemical reaction
α_A Order of reaction for anhydrite dissolution
α_G Order of reaction for gypsum precipitation
Λ Dimensionless parameter
$\bar{\Lambda}$ Dimensionless parameter
Λ^* Dimensionless parameter
Φ Volume fraction
ϕ_A Anhydrite volume fraction
ϕ_{A0} Initial anhydrite volume fraction
$\phi_{A0,crit}$ Critical initial anhydrite volume fraction
ϕ_G Gypsum volume fraction
ϕ_{G0} Initial gypsum volume fraction
$\phi_{G,A}$ Volume fraction of gypsum grown on anhydrite particles
$\phi_{G,G}$ Volume fraction of gypsum grown on gypsum particles
$\phi_{G,S}$ Volume fraction of gypsum grown on inert solid particles
ϕ_P Volume fraction of particles consisting of inert solid and gypsum
ϕ_S Inert solid volume fraction
ϕ_W Water volume fraction
ϕ_{W0} Initial water volume fraction
ρ Density
ρ_A Anhydrite density
ρ_G Gypsum density
ρ_S Inert solid density
ρ_W Water density
τ Dimensionless time
$\bar{\tau}$ Dimensionless time

1 Introduction

Swelling rocks increase their volume by absorbing water. In tunnelling this leads to a heave of the tunnel floor or to the development of a rock load upon the invert lining (so-called swelling pressure). Tunnelling experience shows that the anhydritic claystones of the Gypsum Keuper formation are particularly problematic in this respect. The Gypsum Keuper has caused serious damage and high repair costs in various tunnels in northwestern Switzerland and southwestern Germany (Amstad and Kovári 2001; Einstein 1996). The most recent case of a tunnel crossing the heavily swelling Gypsum Keuper is that of the Chienberg Tunnel close to Basle in Switzerland. The tunnel was opened in December 2007 and experienced since then a floor heave of about 0.80 m (Fig. 1).

Fig. 1 Heave of the floor beneath the carriageway of the Chienberg Tunnel

Anhydritic claystones consist of a clay matrix with finely distributed particles, veins and layers of anhydrite ($CaSO_4$). The swelling of anhydritic claystones is attributed mainly to the chemical transformation of anhydrite to gypsum ($CaSO_4H_2O$), which leads to an increase in the volume of the sulphate by 61 % (the molar volumes of anhydrite and gypsum are equal to 46 and 74 cm^3, respectively). Water uptake by the clay matrix may also contribute to swelling at least to a certain degree (Anagnostou et al. 2010). Figure 2 shows the occurrences of anhydrite according to Langbein et al. (1982) and a review by Serafeimidis and Anagnostou (2012a). The particles may have an approximately spherical or rather prismatic form, while their size lies within a wide range (from few μm to few cm). The shape and size of the anhydrite particles and layers are important for the specific surface of anhydrite and thus for the evolution of its hydration over time.

The mineral transformations in the anhydrite–gypsum–water system take place via the solution phase: anhydrite dissolves in the pore water; gypsum precipitates from the solution. The direction of the transformation (anhydrite to gypsum or, visa versa, gypsum to anhydrite) depends on whether the equilibrium concentration of the anhydrite is higher or lower than that of the gypsum. The equilibrium concentration c_{eq} of a mineral is defined as the maximum amount of solute that dissolves in a solvent. A mineral dissolves into water until the ionic concentration c of the solution reaches the equilibrium concentration. Afterwards, the mineral exists in equilibrium with the solution. Gypsum (rather than anhydrite) is the thermodynamically stable mineral if its equilibrium concentration ($c_{eq,G}$) is lower than that of anhydrite ($c_{eq,A}$). In this case, the entire anhydrite will be dissolved into water, because the ionic concentration c cannot reach its equilibrium concentration $c_{eq,A}$ (which would stop dissolution). This is because, as soon as the concentration c reaches the gypsum equilibrium concentration $c_{eq,G}$, gypsum starts to precipitate, thus consuming ions and maintaining the ionic concentration c below $c_{eq,A}$.

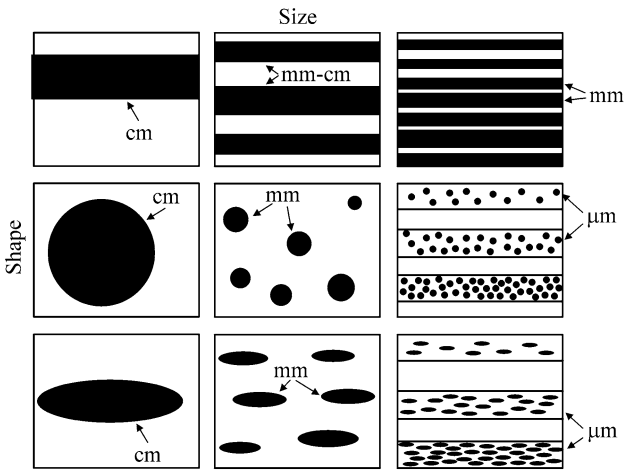

Fig. 2 Classification of anhydrite in natural rocks (after Langbein et al. 1982) and order of the particle size (*left to right* decreasing size, *top to down* different shapes)

The mineral equilibrium concentrations depend in general on the temperature, the pressure and the existence of foreign ions in the solution (see, e.g. Anderson 1996). The equilibrium concentrations of anhydrite and gypsum increase with increasing pressure. At high pressures the equilibrium concentration of gypsum $c_{eq,G}$ is higher than the equilibrium concentration of anhydrite $c_{eq,A}$ with the consequence that gypsum becomes the thermodynamically stable phase. For the pressure range which is relevant at the depths of the tunnels in Gypsum Keuper, the influence of the pressure on the equilibrium concentrations is however very small. Therefore, atmospheric pressure is assumed in the present study. According to the literature, the transition temperature between anhydrite and gypsum is equal to 42–60 °C under atmospheric pressure and in the absence of foreign ions (cf. Freyer and Voigt 2003). Below this transition range, gypsum is the stable phase (i.e. the phase with the lower equilibrium concentration), while above the transition range anhydrite is stable. Under the conditions usually prevailing in tunnelling (nearly atmospheric pressure in the rock around the tunnel, moderate amounts of foreign ions, temperature about 20 °C), gypsum rather than anhydrite represents the thermodynamically stable phase (see equilibrium concentrations in Table 1). Therefore, the chemical process of sulphate hydration (i.e. anhydrite dissolution and gypsum precipitation) is deemed to be one of the most important factors for the swelling of anhydritic rocks.

The setbacks that recur in tunnelling through swelling rock have triggered considerable research efforts into the causes and mechanisms of swelling. A recent overview of the theoretical models for the swelling problem and of recent or ongoing investigations can be found in

Table 1 Assumed parameters (deviations from these values are mentioned in the text)

Parameter	Anhydrite	Gypsum
Densities ρ_A, ρ_G (kg/m^3)	2,960	2,320
Equilibrium concentrations $c_{eq,A}$, $c_{eq,G}$ (mol/m^3)	21.0	15.5
Orders of reactions α_A, α_G (−)	2	2
Reaction rate constants k_A, k_G ($kg/m^2/s$)	3×10^{-6}	5×10^{-7}
Diffusion coefficient $\tilde{k}$ (m^2/s)		8×10^{-10}
Tortuosity T_G (−)		0.66
Porosity of sealing gypsum layer n_G (−)		1.00

Anagnostou et al. (2010). Open questions remain with respect to the role of the chemical reactions and the clay matrix, the effect of the transport processes and the relationship between swelling pressure and swelling strain. In the present contribution we focus on the kinetics of the chemical reactions in sulphatic rocks and, for this reason, we limit ourselves to closed systems, i.e. we do not investigate the effects of seepage flow and diffusive transport, which may also be important. Understanding the factors governing the time-development of anhydrite hydration is an important prerequisite for developing more complex models which take account of transport and chemo-poro-mechanical coupling.

Serafeimidis and Anagnostou (2012a) presented an extended literature review on the kinetic constants of the system anhydrite–gypsum–water including estimations of these parameters by analysing existing experimental results. Furthermore, they investigated the effect of the initial size and shape of the minerals on the time evolution separately for anhydrite dissolution and gypsum precipitation. In a subsequent paper, Serafeimidis and Anagnostou (2012b) investigated the coupled process of simultaneous anhydrite dissolution and gypsum precipitation for spherical and cubical mineral particles.

The present paper brings together and extends the preliminary results of Serafeimidis and Anagnostou (2012a, b) by presenting a more consistent and comprehensive dissolution and precipitation model that accounts for arbitrary geometrical forms of the mineral particles. Special mention is given to the paper of Kontrec et al. (2002), which is the only experimental work on the time-development of the ionic concentration in a closed system consisting of anhydrite, gypsum and water (Sect. 3). In addition, the paper analyzes the important aspect of the sealing of anhydrite by a layer of gypsum, which according to existing investigations (reviewed in Sect. 2.4) might be decisive for the evolution of the hydration process.

The paper begins with a mathematical model for the processes in a closed system taking into account the effect of sealing, emphasising furthermore some of the peculiarities of gypsum precipitation and anhydrite dissolution (Sect. 2). Section 3 checks the predictive capacity of the computational model on the basis of the existing experimental data from Kontrec et al. (2002). Section 4 computationally investigates the effect of the initial composition of the system and of the mineral surface areas involved on the evolution of a closed system over time. It also shows the conditions under which anhydrite dissolution (rather than gypsum precipitation) is the limiting mechanism for the time-development of the hydration process. Section 4 ends by presenting a simplified equation for estimating the duration of the hydration process. The paper finishes with an investigation concerning the effect of the anhydrite surface being sealed by the formation of a gypsum layer (Sect. 5).

2 Dissolution and Precipitation Model

2.1 Mass Balance

Consider a closed system consisting of a solid phase and a liquid phase under isothermal conditions. In the most general case the constituents of the solid phase are anhydrite (A), gypsum (G) and inert minerals (S), i.e. minerals which do not participate in any chemical reaction (e.g. dolomite). The liquid phase contains water (W) and calcium and sulphate ions (I). The mass m_i of the i-th constituent per unit volume of mixture is defined as:

$$m_i = M_i / V_{\text{tot}}, \tag{1}$$

where the subscript i refers to the constituent (i = A, G, W, S or I); M_i (kg) denotes the mass of the i-th constituent at a given time and V_{tot} (m^3) is the volume of the mixture (for small volume changes, V_{tot} can be taken approximately equal to the initial mixture volume $V_{\text{tot},0}$). The volume fractions ϕ_i of the mixture constituents are given by:

$$\phi_i = V_i / V_{\text{tot}} = m_i / \rho_i, \tag{2}$$

where V_i and ρ_i are the volume and the density of the constituent i, respectively. The term ϕ_{w} thus represents the porosity of the medium. The sum of the volume fractions ϕ_i should obviously equal unity at any time. The ion concentration c is important for calculating the reaction rates (see Sect. 2.2) and can be expressed as a function of the ion and water masses per unit volume as follows:

$$c = M_{\text{I}} / V_{\text{W}} = \rho_{\text{W}} m_{\text{I}} / m_{\text{W}}. \tag{3}$$

In a closed system, masses change only due to chemical reactions. The chemical reactions and masses involved in the present case are the following:

$$\begin{array}{ccc} \text{CaSO}_4 & \longrightarrow & \text{Ca}^{2+} + \text{SO}_4^{2-} \\ 0.136\text{kg/mol} & & 0.136\text{kg/mol} \end{array} \tag{4}$$

and

$$\begin{array}{ccccc} \text{Ca}^{2+} + \text{SO}_4^{2-} & + \ 2\text{H}_2\text{O} & \longrightarrow & \text{CaSO}_4 \cdot 2\text{H}_2\text{O} \\ 0.136\text{kg/mol} & 0.036\text{kg/mol} & & 0.172\text{kg/mol} \end{array} \tag{5}$$

The ion concentration therefore increases due to anhydrite dissolution (Eq. 4), while the concentration and water content decrease due to gypsum precipitation (Eq. 5). The mass balance equation for the ions and the water therefore read as follows:

$$m_{\text{I}} = m_{\text{I}0} + (m_{\text{A}0} - m_{\text{A}}) - 136(m_{\text{G}} - m_{\text{G}0})/172 \tag{6}$$

and

$$m_W = m_{W0} - 36(m_G - m_{G0})/172, \quad (7)$$

where m_{A0}, m_{W0}, m_{G0} and m_{I0} denote the initial masses per unit volume.

2.2 Fundamentals of Dissolution and Precipitation Reaction Kinetics

Different formulations can be found in the literature for dissolution and precipitation rates (e.g. Appelo and Postma 2005; Lasaga 1986, 1998; Mullin 2001; Nancollas and Purdie 1964; Steefel and Van Cappellen 1990; Steefel and Lasaga 1994). Generally, the rates depend on the reactive surface area of the mineral, the temperature and the distance of the system from thermodynamic equilibrium.

A general formulation for the mass change rate of a mineral in contact with water due to dissolution or precipitation is (Mullin 2001):

$$dM/dt = kAf(c), \quad (8)$$

where dM/dt (kg/s) is the mass change rate of the mineral (positive for precipitation and negative for dissolution); A (m^2) denotes the surface area of the mineral in contact with water (note that A may vary over time); k ($kg/m^2/s$) is the reaction rate constant (increases with temperature according to the equation of Arrhenius, cf., e.g. Atkins and De Paula 2006); and $f(c)$ is a function of the ion concentration c. It is given here as a function of the relative supersaturation (Mullin 2001):

$$f(c) = \mathrm{sgn}(c - c_{eq}) \cdot \left|(c - c_{eq})/c_{eq}\right|^a, \quad (9)$$

where α represents the order of the chemical reaction, c_{eq} is the equilibrium concentration of the mineral and, consequently $(c - c_{eq})/c_{eq}$ expresses the degree of oversaturation, i.e. the driving force for dissolution and precipitation. For solutions that are supersaturated with respect to the mineral, i.e. for $c > c_{eq}$, $f(c)$ and the mass change rate are therefore also positive and precipitation takes place. On the other hand, in the case of undersaturated solutions ($c < c_{eq}$), the mass change rate is negative and the mineral dissolves.

Serafeimidis and Anagnostou (2012a) presented a comprehensive review of the kinetic constants of anhydrite dissolution and gypsum precipitation: Both reactions are of second order (i.e. $\alpha = 2$), while the reaction rate constants are $k_A = 0.54\text{–}5.4 \times 10^{-6}$ $kg/m^2/s$ for anhydrite dissolution and $k_G = 5.19 \times 10^{-7}\text{–}5.35 \times 10^{-6}$ $kg/m^2/s$ for gypsum precipitation.

From Eqs. (1), (2) and (8), we obtain the following equation for the mass change of a mineral per unit volume of the mixture:

$$\frac{dm}{dt} = \rho \frac{d\phi}{dt} = k\,\phi\,F f(c), \quad (10)$$

where F (m^{-1}) is the specific surface area of the mineral, while the product of ϕ by F is equal to the surface area of the dissolving or precipitating mineral per unit volume of the mixture.

Alternatively, the dissolution and precipitation rates can be expressed in terms of the distance s of the surface of a mineral at time t from the initial mineral surface (see Fig. 3 for the definition and the sign of s). Equation (8) is equivalent to the following equation for the rate of s:

$$\frac{ds}{dt} = \frac{k}{\rho} f(c), \quad (11)$$

where $f(c)$ is given by Eq. (9). For mineral dissolution, $f(c) < 0$ and consequently s decreases, while for mineral precipitation $f(c) > 0$ and s increases.

2.3 Peculiarities of the Precipitation Process

In the case of mineral dissolution, the surface area A appearing in Eq. (8) is always clearly defined: it is equal to the surface area of the mineral that is in contact with water and thus available for dissolution. On the other hand, the precipitation of a mineral that is absent from the system initially presents the problem that its initial surface area A is equal to zero. Since precipitation according to Eq. (8) cannot start if $A = 0$, the non-existence of an initial surface area A introduces inherent difficulties and uncertainties to modelling. According to the theory of nucleation (Lasaga 1998; Mullin 2001), crystallisation nuclei are formed after a certain induction time when the solution becomes supersaturated, and subsequent crystal growth takes place on these nuclei. Nucleation is a very complex process. Attempts to bypass this process in modelling by simplified assumptions introduce large uncertainties (Steefel and Lasaga 1994; Lasaga and Rye 1993). However, it is not necessary to consider the nucleation process explicitly in the present study, because natural systems contain a lot of impurities or foreign crystals, which serve as crystallisation nuclei (Mullin 2001).

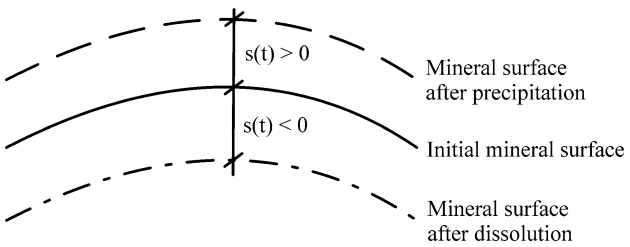

Fig. 3 Movement of mineral surface area due to dissolution or precipitation

The rate of the increase of the gypsum mass depends also on the area A of the surface on which crystal growth occurs (Eq. 8). Gypsum crystals grow either on pre-existing gypsum particles or veins, or on other rock minerals. Although there are several techniques which in principle allow the mineral surface to be investigated and quantified (Brantley et al. 2008), determination of this surface is in practical terms difficult for natural rocks, particularly when considering that the surfaces of some minerals (e.g. gypsum particles) will be more likely sites of precipitation than the surfaces of other minerals. Normally, one makes an a priori assumption regarding the initial surface area (Steefel and Lasaga 1994; Lasaga and Rye 1993; Mäder, personal communication). Nevertheless, this assumption is not critical because in water–rock interaction systems, where both dissolution and precipitation take place, the time evolution of the process is governed by dissolution, i.e. the hydration develops close to the equilibrium of the precipitating mineral (Mäder, personal communication). This means that the rates of mineral mass growth due to precipitation are much higher than the rates of mineral mass decrease due to dissolution and, therefore, it is often sufficient for modelling to make the simplifying assumption of a large initial value for the surface on which precipitation occurs. The conditions under which this simplifying assumption is reasonable (i.e. the conditions under which anhydrite dissolution represents the limiting mechanism) are investigated in Sect. 4.3.

2.4 Sealing of Anhydrite by the Formed Gypsum Layer

In general, gypsum growth may also take place on the anhydrite surface, forming a layer of gradually increasing thickness. According to Böhringer et al. (1990), this happens within a few months. The gypsum layer can be up to a few millimetres thick and may (depending on its thickness and porosity) slow down or even stop anhydrite dissolution, because the dissolving ions must diffuse through this layer in order to reach the macropores. At the same time, the gypsum seals the anhydrite by clogging communicating pores and fissures, which also leads to a significant deceleration or even halt in the anhydrite dissolution and thus also in the hydration process (Müller and Briegel 1977). This is why massive anhydrite, i.e. compact rock consisting mainly of anhydrite, does not swell. Amstad and Kovári (2001) concluded, on the basis of a synthesis of different observations that anhydrite layers do not swell within the usual service life of tunnels (100 years) if they are thicker than 20 mm.

The sealing effect of gypsum was noticed already by Wiesmann (1914) during the construction of Hauenstein Basetunnel in Switzerland. Similar observations were made in the Simplon tunnel, in which massive anhydrite with some insignificant dolomite inclusions was encountered in the bottom adit over a 100 m long section (Amstad and Kovári 2001). According to Andreae (1956), this part of the adit (9.7–9.8 km from the northern portal) remained unlined for about 10 years. However, no swelling was observed although the relative humidity of the air was practically 100 %, due to a nearby steamy natural hot water well. Gassmann et al. (1979) mentioned that anhydrite sealing was also observed at the tunnel walls and in boreholes in the exploration gallery Val Canaria. Existing fissures were sealed by a gypsum layer within 50 years. Additional evidence on the negligible swelling potential of massive anhydrite can be found in a number of South German tunnels crossing the Gypsum Keuper (Grob 1972; Henke and Kaiser 1975; Henke et al. 1975).

Similar observations were made by Sahores (1962) who investigated masonry built with anhydrite quarry stones. The masonry had remained in very good condition although it was exposed to temperature changes and rainwater for more than 50 years. Sahores (1962) attributed this to a thin gypsum layer formed on the surface of the anhydrite blocks and checked this hypothesis by means of laboratory tests.

Madsen and Nüesch (1990) experimentally investigated the behaviour of massive anhydrite from the Weiach borehole. After almost 2 years of testing, rock samples consisting of 99 wt% anhydrite and 1 wt% clay and carbonate, developed swelling pressures of up to 0.05 MPa and swelling strains of up to 1 % only. These figures are negligible relative to those of claystones with finely distributed anhydrite, which exhibit swelling pressures and strains of up to 7–8 MPa and up to 30–40 %, respectively.

We model here the sealing effect of the gypsum layer similar to Bezjak and Jelenic (1980), Pignat et al. (2005) and Bishnoi and Scrivener (2009), who investigated the transformation of tricalcium silicate (C_3S) to calcium silicate hydrate (C–S–H) in the context of cement technology. The similarity to the sealing effect of gypsum is due to the fact that diffusion through the C–S–H layer (which covers the C_3S grains) represents—besides nucleation/growth and phase boundary reactions—one of the mechanisms which govern the time evolution of the C_3S hydration.

In the absence of a gypsum sealing layer, anhydrite dissolution would occur according to Eqs. (9) and (11), i.e. the dissolution front would move with the following rate:

$$\frac{\mathrm{d}s_\mathrm{A}}{\mathrm{d}t}\Big|_\mathrm{DIS} = -\frac{k_A}{\rho_A}\left(\frac{c_\mathrm{eq,A}-c}{c_\mathrm{eq,A}}\right)^{\alpha_\mathrm{A}}. \tag{12}$$

The sealing effect of the gypsum layer on anhydrite dissolution can be taken into account by considering that the diffusive flow of the calcium and sulphate ions through

the gypsum may be the limiting mechanism. According to Fick's law, the diffusive flux

$$J = -\tilde{k}\, n_G\, T_G \frac{c - c_{eq,A}}{s_G}, \tag{13}$$

where $\tilde{k}$ (m^2/s), T_G (−), n_G (−) and s_G (m) denote the diffusion coefficient, the tortuosity, the porosity and the thickness of the gypsum layer, respectively. With increasing thickness of the gypsum layer, the diffusive flow may become slower than the flow predicted by Eq. (8) and may become the decisive factor for the rate of the anhydrite dissolution. In this case, the anhydrite surface will retreat with the following rate:

$$\frac{ds_A}{dt}|_{DIF} = -\frac{J}{\rho_A} = -n_G\, T_G\, \frac{\tilde{k}}{\rho_A} \frac{c_{eq,A} - c}{s_G}. \tag{14}$$

Equation (12) applies for the initial stage of the dissolution process, i.e. as long as it leads to lower values than Eq. (14). According to Eq. (14), the sealing effect of the gypsum layer depends essentially on how dense this layer is, i.e. on its porosity. Porosity probably decreases over time as increasing numbers of crystals grow. More specifically, a denser layer should develop if gypsum growth in the pore space is constrained (cf., e.g. Bezjak and Jelenic 1980; Bishnoi 2008). As experimental data concerning this matter do not exist, we make here the simplifying assumption of a constant porosity n_G and investigate its effect quantitatively.

2.5 Governing Equations

From Eqs. (9), (11), (12) and (14), the following dimensionless relationships can be obtained for the movement rate of the dissolution and precipitation front s_A and s_G, respectively:

$$\frac{d\bar{s}_A}{d\bar{\tau}} = -\min\left[(1-\tilde{c})^{a_A};\, n_G T_G \frac{\tilde{k}}{k_A} \frac{c_{eq,A}}{S_{A0}\bar{s}_G}(1-\tilde{c})\right] \tag{15}$$

and

$$\frac{d\bar{s}_G}{d\bar{\tau}} = \bar{\Lambda}\left(\frac{\tilde{c}}{\tilde{c}_{eq,G}} - 1\right)^{a_G} \frac{1}{1-n_G}, \tag{16}$$

where

$$\tilde{c} = c/c_{eq,A}, \tag{17}$$

$$\tilde{c}_{eq,G} = c_{eq,G}/c_{eq,A}, \tag{18}$$

$$\bar{\tau} = \frac{k_A}{S_{A0}\rho_A} t, \tag{19}$$

$$\bar{\Lambda} = \frac{k_G}{k_A}\frac{\rho_A}{\rho_G}, \tag{20}$$

$$\bar{s}_A = s_A/S_{A0} \tag{21}$$

and

$$\bar{s}_G = s_G/S_{A0}. \tag{22}$$

The last term in Eq. (16) accounts for the porosity of the sealing layer (Sect. 2.4). The variable $\bar{\tau}$ denotes a dimensionless time, while S_{A0} is a characteristic length (e.g. the initial diameter of the anhydrite particles in the case of spherical anhydrite particles) used here for normalizing s_A and s_G.

Equation (15) only applies under the following conditions:

$$c < c_{eq,A}, \quad \phi_A > 0, \quad \phi_G < \frac{172}{36}\frac{\rho_W}{\rho_G}\phi_{W0} + \phi_{G0}. \tag{23}$$

The last inequality follows from the condition $\phi_W > 0$ and Eqs. (2) and (7). It must also be fulfilled (in addition to $c > c_{eq,G}$) due to Eq. (16).

Equations (15) and (16) are coupled via the dimensionless concentration $\tilde{c}$. From Eqs. (3), (6) and (7) we obtain $\tilde{c}$ as a function of the volume fractions of anhydrite and gypsum:

$$\tilde{c} = \tilde{c}_0 \frac{\phi_{W0}}{\phi_W} + \frac{\rho_A}{c_{eq,A}} \frac{\phi_{A0} - \phi_A - \frac{136}{172}\frac{\rho_G}{\rho_A}\phi_G}{\phi_W}, \tag{24}$$

where the porosity

$$\phi_W = \phi_{W0} - \frac{36}{172}\frac{\rho_G}{\rho_W}\phi_G, \tag{25}$$

the initial porosity

$$\phi_{W0} = 1 - \phi_{A0} - \phi_{G0} - \phi_S \tag{26}$$

and

$$\tilde{c}_0 = c_0/c_{eq,A}. \tag{27}$$

In order to calculate the concentration c with Eq. (24), the volume fractions of anhydrite and gypsum are needed. These depend on the shape and size of the anhydrite and gypsum particles and thus on the thicknesses, s_A and s_G. Two shapes for the mineral particles will be considered here: parallelepipeds and spheres. The initial side lengths of the parallelepipeds are S_0, aS_0 and bS_0 (Fig. 4a), while the spherical particles have an initial diameter S_0 (Fig. 4b). The characteristic length S_{A0} used for normalizing s_A and s_G is thus equal to the initial particle diameter (in the case of spherical anhydrite particles) or to the smallest side length if the anhydrite occurs in the form of parallelepipeds.

Gypsum may grow on pre-existing gypsum particles, on anhydrite particles or on other inert minerals. The volume fraction of gypsum ϕ_G therefore consists of the initial fraction ϕ_{G0} and three additional terms:

$$\phi_G = \phi_{G0} + \phi_{G,G} + \phi_{G,A} + \phi_{G,S}, \tag{28}$$

where $\phi_{G,G}$, $\phi_{G,A}$ and $\phi_{G,S}$ are the volume fractions of the gypsum that precipitates on gypsum, anhydrite and on

other solids, respectively. For simplicity we assume here that gypsum growth occurs at the same rate on all particles in the system under consideration.

The geometric relationships expressing the volume fractions ϕ_A, $\phi_{G,G}$, $\phi_{G,S}$ and $\phi_{G,A}$ in terms of the primary variables s_A and s_G are given in the "Appendix".

3 Model Check

The model in Sect. 2 was tested by taking into account the results of Kontrec et al. (2002), who performed experiments on the dissolution of anhydrite, on the precipitation of gypsum as well as on the simultaneous anhydrite dissolution and gypsum precipitation. They investigated also the dissolution of gypsum, which is nonetheless out of the scope of the present study.

Kontrec et al. (2002) performed also a back analysis of their experiments, however, without giving the complete mathematical formulation of their model. More specifically, they presented the equations for anhydrite dissolution and gypsum precipitation, but not the equations needed for the simultaneous process. Furthermore, their equations apply for spherical or cubical particles only, despite the fact that the used anhydrite particles had an irregular shape and the gypsum particles were platelets. Moreover, the rate constants used in their work were not material specific but applied only to the particles sizes considered. The model of the present work (Sect. 2) is more general in that it considers different particle shapes and accounts explicitly for their specific surface area. In spite of the uncertainties that exist with respect to the mathematical formulation used by Kontrec et al. (2002), their model must be similar to the present model as it leads to similar predictions.

In the absence of information concerning the particle shape of anhydrite, spherical particles are assumed for the calculations with the corresponding surface area (3.78 m^2/g). Gypsum particles are elongated platelets with approximate proportions 21:8:2 and a specific surface area of 0.3 m^2/g. Table 1 shows the orders of reactions used as well as the rate constants of the anhydrite dissolution and gypsum precipitation.

The first test used to check the model concerns the dissolution of anhydrite for three different initial masses of anhydrite in the solution (m_{A0} = 1.60, 2.28, 4.00 kg/m^3). The initial ion concentration was 15.5 mol/m^3, i.e. equal to the equilibrium concentration of gypsum (cf. Table 1). Figure 5a shows the computed ion concentration (solid line) over time and the measured values. The computational results agree in general with the experimental results of Kontrec et al. (2002), nonetheless with some deviations which can be attributed to the uncertainty due to the particle shape, as mentioned before.

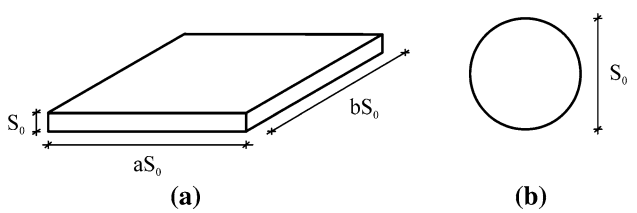

Fig. 4 **a** Parallelepipedic and **b** spherical particle

The second test concerns the precipitation of gypsum with an initial mass of m_{G0} = 2.28 kg/m^3 and initial ion concentration c_0 = 33 mol/m^3. Figure 5b depicts the computed ion concentration (solid line) as a function of time. The measured values (dots) correspond to a temperature of 20 °C. The model check was performed for these values, despite the fact that Kontrec et al. (2002) provided measured values for different temperatures as well, since the reaction rate constants of Table 1 have been derived for temperatures around 20 °C (cf. Serafeimidis and Anagnostou 2012a). In this case a good correlation between the results exists.

Finally, the model of the present paper (Sect. 2) was tested by taking into account the experimental results for simultaneous anhydrite dissolution and gypsum precipitation. In the test under consideration, the initial anhydrite and gypsum masses in the solution were equal ($m_{A0} = m_{G0}$ = 2.312 kg/m^3). The initial ion concentration c_0 was 16 mol/m^3, i.e. slightly higher than the equilibrium concentration of gypsum (cf. Table 1).

Figure 5c shows the computed ion concentration over time (solid line) and the measured values (dots). The computational results agree to a great extent with experimental results from Kontrec et al. (2002) (the uncertainty due to the anhydrite particle shape should be considered also in this case). The distinct non-linearity obtained in the concentration over time can be explained as follows: At the very initial stage of the process, the concentration is close to the equilibrium concentration of gypsum and therefore only anhydrite dissolution takes place. Consequently, a steep increase in the concentration is observed. The effect of the increasing concentration is twofold: On the one hand, anhydrite dissolution slows down due to the fact that the difference between the actual concentration and the equilibrium concentration of anhydrite decreases. On the other hand, as the solution becomes increasingly oversaturated with respect to gypsum, crystal growth starts to occur and consume ions. The concentration reaches therefore a maximum and decreases thereafter. The second characteristic feature of the curve of concentration over time is the turning point at approximately t = 33 h. The turning point marks the termination of the anhydrite dissolution process (Fig. 5d).

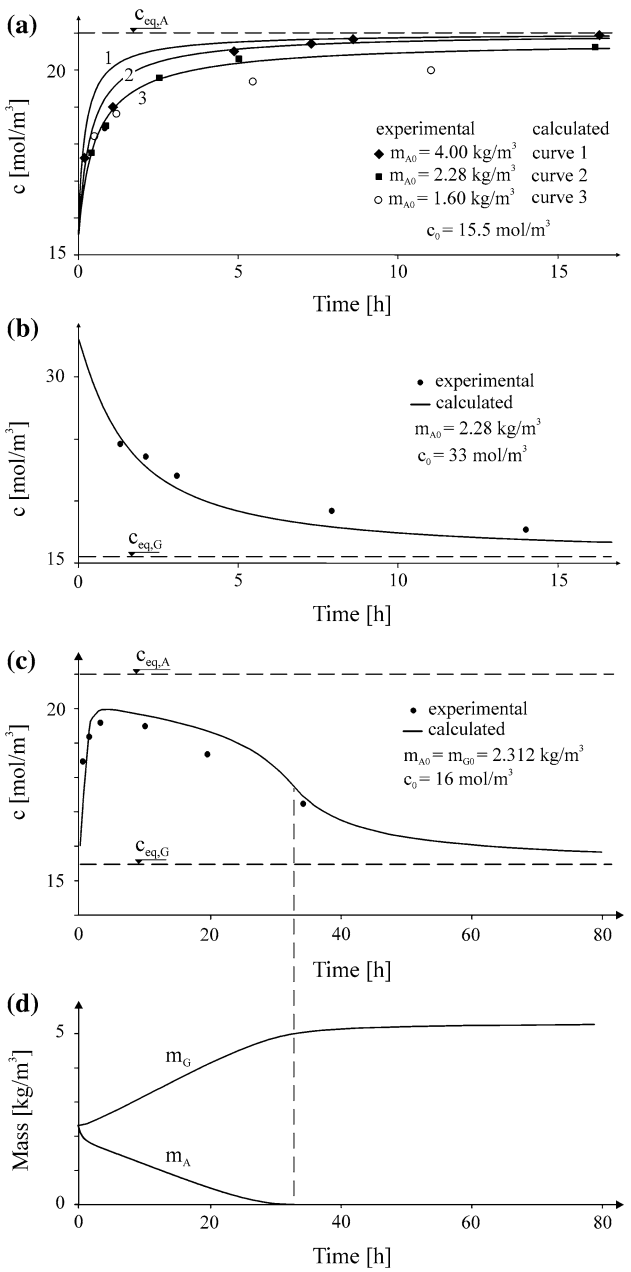

Fig. 5 Back-analysis of the experimental data by Kontrec et al. (2002)—ion concentration over time for the following processes: **a** anhydrite dissolution, **b** gypsum precipitation, **c** simultaneous anhydrite dissolution and gypsum precipitation and **d** anhydrite and gypsum mass over time

4 Parametric Study on the Time-Development of Hydration

4.1 Introduction

The present section discusses the results of parametric studies for a porous medium with gypsum growth on inert minerals (no sealing of anhydrite). For this special case, it is advantageous to formulate the governing equations in terms of the volume fractions of anhydrite and gypsum instead of s_A and s_G. From Eq. (10) we obtain:

$$\frac{d\phi_A}{d\tau} = -\frac{\phi_A F_A}{\phi_{A0} F_{A0}} (1-\tilde{c})^{a_A}, \tag{29}$$

$$\frac{d\phi_G}{d\tau} = \Lambda \frac{\phi_P F_P}{\phi_S F_S} \left(\frac{\tilde{c}}{\tilde{c}_{eq,G}} - 1 \right)^{a_G}, \tag{30}$$

where the dimensionless parameter

$$\Lambda = \frac{k_G}{k_A} \frac{F_S}{F_{A0}} \frac{\phi_S}{\phi_{A0}} \frac{\rho_A}{\rho_G} \tag{31}$$

and expresses how quickly gypsum precipitation occurs relative to anhydrite dissolution (i.e. it is a measure of the relative speed of the two processes), while the dimensionless time is:

$$\tau = t \, \frac{k_A F_{A0}}{\rho_A} \phi_{A0}. \tag{32}$$

The symbols ϕ_P and F_P denote the volume fraction and the specific surface area of the particles that are available for gypsum precipitation (inert mineral with formed gypsum on it). At $t = 0$, ϕ_P and F_P are equal to the volume fraction ϕ_S and to the specific surface F_S of the inert particles, respectively.

In general, F_A and F_P change with time and are related to ϕ_A and ϕ_P in a more or less complex way, depending on the shape of the particles. The advantage of the formulation of Sect. 2.5 is that it allows for a more consistent treatment of different particle shapes and of different precipitation cases (precipitation on gypsum, on inert minerals and on anhydrite). However, the formulation of the current section is useful, particularly for the case of spherical particles, because in this special case the equations simplify considerably. More specifically, for spherical particles, Eqs. (29) and (30) take the following form:

$$\frac{d\phi_A}{d\tau} = -\left(\frac{\phi_A}{\phi_{A0}} \right)^{2/3} (1-\tilde{c})^{a_A} \tag{33}$$

and

$$\frac{d\phi_G}{d\tau} = \Lambda \left(1 + \frac{\phi_G}{\phi_S} \right)^{2/3} \left(\frac{\tilde{c}}{\tilde{c}_{eq,G}} - 1 \right)^{a_G}. \tag{34}$$

Equations (33) and (34), with the concentration $\tilde{c}$ according to Eq. (24), represent a system of two nonlinear ordinary differential equations for the evolution of the volume fractions of anhydrite and gypsum over time. The solution of this system can be expressed as follows:

$$\phi_A,\ \phi_G,\ \phi_W,\ \frac{c}{c_{eq,A}} = f\left(\tau,\ \Lambda,\ \phi_{A0},\ \phi_{W0},\ \frac{c_0}{c_{eq,A}},\ \frac{c_{eq,G}}{c_{eq,A}},\ \frac{c_{eq,A}}{\rho_A},\ \frac{\rho_G}{\rho_A},\ \frac{\rho_G}{\rho_W} \right). \tag{35}$$

The equations of this section apply also to the case where gypsum growth occurs on gypsum particles that pre-exist in the system (the only difference being that ϕ_P, F_P, ϕ_S and F_S should be replaced by ϕ_G, F_G, ϕ_{G0} and F_{G0}, respectively).

4.2 Evolution Over Time

We investigate the time-development of hydration by means of a parametric study concerning mixtures consisting initially of anhydrite, inert minerals and distilled water ($c_0 = 0$ mol/m^3). For simplicity, all particles are assumed to be spherical and therefore Eqs. (33) and (34) can be used.

The last five parameters on the right hand side of Eq. (35) represent material constants. Furthermore, in the investigations of the present Section, the initial water content ϕ_{W0} will be kept equal to 0.15. Therefore, the evolution of the hydration process over time (represented by the dimensionless time τ) is governed only by the dimensionless parameter Λ and by the initial anhydrite fraction ϕ_{A0} (cf. Eq. 35).

During the hydration process, the pore water may be consumed while anhydrite is still present in the system. Hydration of the entire anhydrite presupposes the presence of sufficient water or, for a given water content, that the anhydrite content does not exceed a critical value. The following relationship gives the critical volume fraction of anhydrite:

$$\phi_{A0,crit} = \frac{136}{36}\frac{\rho_W}{\rho_A}\phi_{W0} \cong 1.276\,\phi_{W0}. \tag{36}$$

For the assumed initial water content $\phi_{W0} = 0.15$, hydration will end prematurely if the anhydrite content exceeds $\phi_{A0,crit} = 0.19$.

Figure 6a and b show the ion concentration and the volume fraction of anhydrite, respectively, over the dimensionless time τ, for $\Lambda = 1$ and initial anhydrite contents ϕ_{A0} of 7.7, 14.2, 28.3 or 42.5 %. In the last two cases, hydration remains incomplete due to consumption of the whole amount of water. It is interesting that the maximum concentration attained during the process does not depend on the initial anhydrite fraction (all curves in Fig. 6a reach the same maximum). As all ϕ_{A0} over τ curves exhibit about the same gradient (Fig. 6b), the initial anhydrite content ϕ_{A0} determines the time needed for the system to reach equilibrium: The duration of the process increases practically linearly with ϕ_{A0}.

The diagrams in Fig. 6c, d show the time-development of the concentration c and of the volume fraction of anhydrite ϕ_A, respectively, for a fixed initial mixture composition. Every curve corresponds to another value of the dimensionless parameter Λ. This parameter expresses the speed of gypsum formation relative to anhydrite dissolution. At high values of Λ, gypsum crystals grow much more quickly than anhydrite dissolves and, consequently, the ion consumption (which is associated with gypsum formation) occurs rapidly relative to the ion production by anhydrite dissolution. Therefore, the concentration cannot increase very much and remains slightly above the equilibrium concentration of gypsum (see curve for $\Lambda = 10$ in Fig. 6c). On the other hand, for low values of Λ, the precipitation of gypsum and the consumption of ions occur relatively slowly. In this case, anhydrite dissolution causes a pronounced oversaturation with respect to gypsum (Fig. 6c). It is therefore evident that the value of the dimensionless parameter Λ determines the maximum value of the concentration c_{max}: The higher the parameter Λ, the lower the maximum oversaturation with respect to gypsum will be.

In conclusion, the anhydrite content determines the duration of the hydration process for a given value of Λ, while Λ determines whether the process is dissolution- or precipitation-controlled. These results also remain valid for other mixture compositions, including dilute aqueous solutions (Serafeimidis and Anagnostou 2012b).

4.3 Limiting Mechanism

As mentioned earlier, the maximum concentration c_{max} shows whether anhydrite dissolution or gypsum precipitation will determine the duration of the hydration process. If anhydrite dissolution represents the limiting mechanism, the concentration is close to the equilibrium concentration of gypsum. On the other hand, the concentration reaches values closer to the saturation concentration of anhydrite if the process is governed by the precipitation of gypsum.

As explained in Sect. 3, a steep increase in the concentration can be observed at the beginning of the process, where anhydrite dissolution alone takes place (Fig. 6a, c). The increasing concentration slows down anhydrite dissolution and accelerates gypsum growth with the consequence that the curve of concentration over time exhibits a maximum.

Figure 6c indicates that the maximum concentration c_{max} depends solely on the dimensionless parameter Λ. This can also be shown on the governing equations. Taking into account the fact that the quantity of anhydrite that has to be dissolved in order for c_{max} to be reached is so low that $\phi_A = \phi_{A0}$, $F_A = F_{A0}$ and $\phi_G = 0$ can be assumed in Eqs. (29) and (30), the condition $dc/dt = 0$ (which applies when $c = c_{max}$) leads to an algebraic equation for c_{max}, whose solution reads as follows:

$$c_{max} = c_{eq,G}\frac{\Lambda^* + 1}{\Lambda^* + c_{eq,G}/c_{eq,A}}. \tag{37}$$

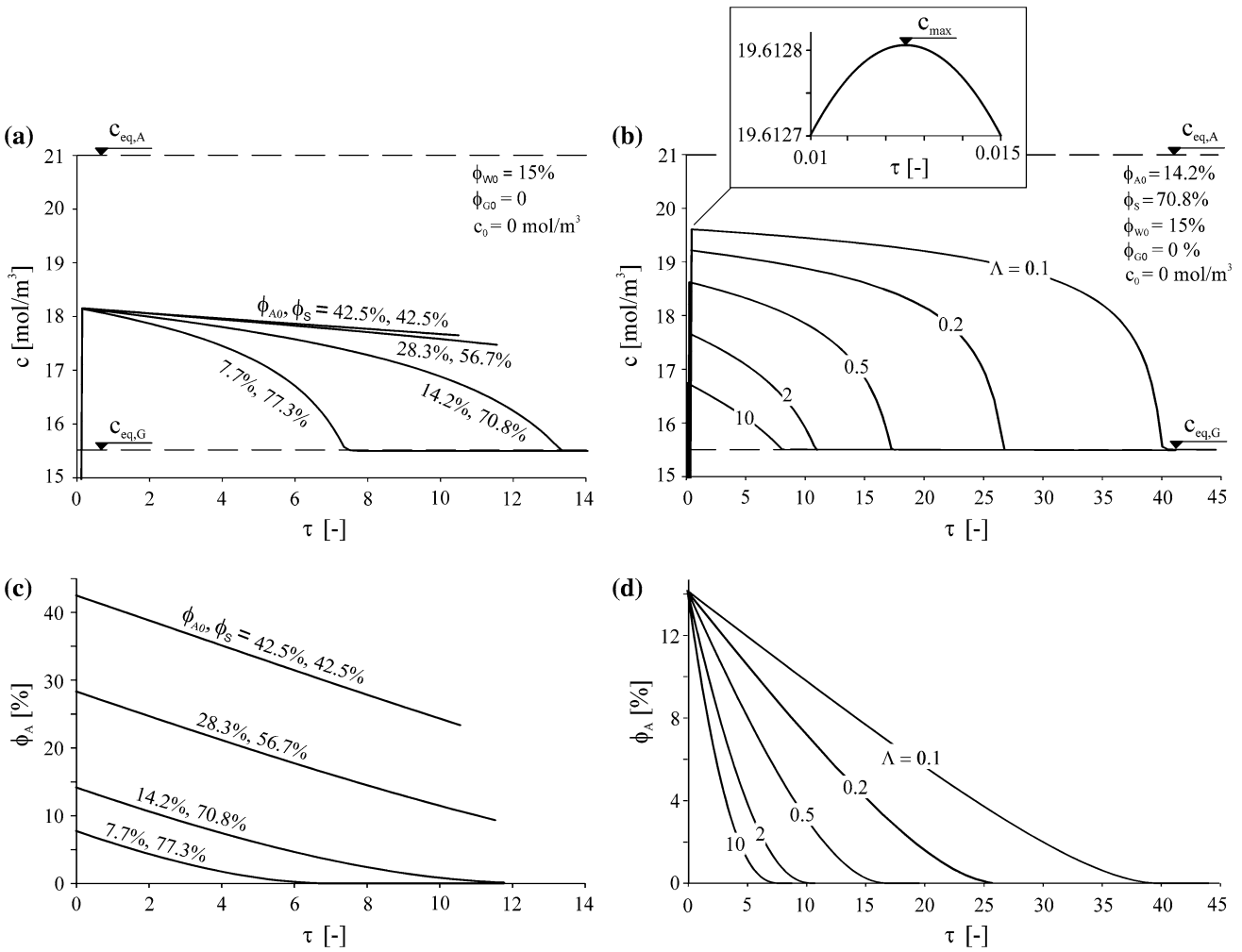

Fig. 6 **a** Ion concentration c and, **b** volume fraction of anhydrite ϕ_A over dimensionless time τ for different initial anhydrite fractions ϕ_{A0}. **c** Ion concentration c and, **d** volume fraction of anhydrite ϕ_A over dimensionless time τ for different values of the dimensionless parameter Λ

where

$$\Lambda^* = \sqrt{\frac{136}{172}\frac{\rho_G}{\rho_A}}\Lambda = \sqrt{\frac{136}{172}\frac{k_G}{k_A}\frac{F_S}{F_{A0}}\frac{\phi_S}{\phi_{A0}}}. \tag{38}$$

This equation confirms that the maximum concentration c_{max} that develops during the hydration process depends solely on the dimensionless parameter Λ. Figure 7 shows the maximum concentration c_{max} as a function of Λ (the abscissa contains additionally the term $F_s\phi_s/F_{A0}\phi_{A0}$). It can be seen that for high Λ-values, i.e. for rapid gypsum precipitation, the c_{max}-values are only slightly higher than the equilibrium concentration of gypsum $c_{eq,G}$. In this case, anhydrite dissolution constitutes the limiting mechanism. On the other hand, for very low values of Λ, the maximum concentration c_{max} approaches the equilibrium concentration of anhydrite $c_{eq,A}$. In this case, the gypsum precipitation is considerably slower than the anhydrite dissolution and governs the time-development of the hydration process.

In general, the process occurs close to gypsum equilibrium (i.e. its time-development is controlled by the dissolution of anhydrite) when Λ is higher than about 5 (Serafeimidis and Anagnostou 2012b). Taking into account the definition of Λ (Eq. 31), this criterion leads to the following inequality:

$$F_{A0}\phi_{A0} < \frac{k_G\rho_A}{5k_A\rho_G}F_S\phi_S. \tag{39}$$

Figure 8 graphically represents this condition. The two lines correspond to extreme combinations of the reaction rate constants for anhydrite dissolution and gypsum precipitation found in the literature (cf. Serafeimidis and Anagnostou 2012a). Points below the lower line do certainly satisfy Eq. (39), thus indicating conditions under which the dissolution of anhydrite constitutes the limiting mechanism. For points lying between the upper and the lower line, it is not possible to make a clear statement about the limiting mechanisms due to the

uncertainty related to the rate constants. According to Fig. 8, anhydrite dissolution governs the overall process, if the anhydrite surface area $\phi_{A0} F_{A0}$ amounts to a maximum 10–100 m^2/m^3 of rock. For instance, this is true in the case anhydrite is in the form of at least 10 mm thick veins, spaced at about 200 mm, and gypsum crystals grow on spherical particles with a maximum radius of 1 mm (point A in Fig. 8).

4.4 Duration of the Hydration Process

According to Fig. 6b, after the very short initial period of rapidly increasing concentration, the volume fraction of anhydrite decreases at an approximately constant rate that does not depend on ϕ_S/ϕ_{A0} over a long period of time. This rate can be derived from Eq. (29), by substituting $\phi_A \cong \phi_{A0}$, $F_A = F_{A0}$ and $c \cong c_{max}$. Assuming the presence of a sufficient quantity of water (i.e., that $\phi_{A0} < \phi_{A0,crit}$), we obtain the following approximation for the hydration time:

$$t_h \cong \frac{\rho_A}{k_A F_{A0}} \left(\frac{c_{eq,A}}{c_{eq,A} - c_{eq,G}} \right)^2 \left(1 + \frac{c_{eq,G}/c_{eq,A}}{\Lambda^*} \right)^2 . \qquad (40)$$

Due to the slight curvature of the ϕ_A over τ curve, this equation gives the lower bound of the hydration time. Figure 9 is based on Eq. (40) and shows the hydration time t_h as a function of the initial specific surface area (F_{A0}) of the anhydritic particles for different ratios of the initial surface areas $\phi_{A0}F_{A0}/\phi_S F_S$. Depending on the initial specific surface area of the anhydrite F_{A0} and on the available surface area for gypsum precipitation $\phi_S F_S$, hydration takes from few hours to several years.

If the process is dissolution-controlled (i.e. for large Λ values), the last right hand side term of Eq. (40) becomes equal to 1. The hydration time is then inversely proportional to the specific surface of anhydrite F_{A0} and does not depend on its volume fraction ϕ_{A0}. This result emphasises the importance of anhydrite distribution with respect to the intensity of swelling. For the cases of practical interest where $\Lambda > 5$, the parameter values of Table 1 and anhydrite particle radii of 0.1–10 mm, one obtains from Eq. (40) hydration times between 5 days and 18 months. This result does not account for the sealing effect.

5 The Effect of Sealing

As explained in Sect. 2.4, in the presence of a gypsum coating, the kinetics of anhydrite dissolution will be governed by the slowest mechanisms of dissolution and diffusion according to Eqs. (12) and (14), respectively. Figure 10 shows the retreat rate of the dissolution front as a function of the ion concentration c. Curve 5 is the second-order dissolution equation (Eq. 12) for the values of Table 1. The straight lines 1–4 were calculated according

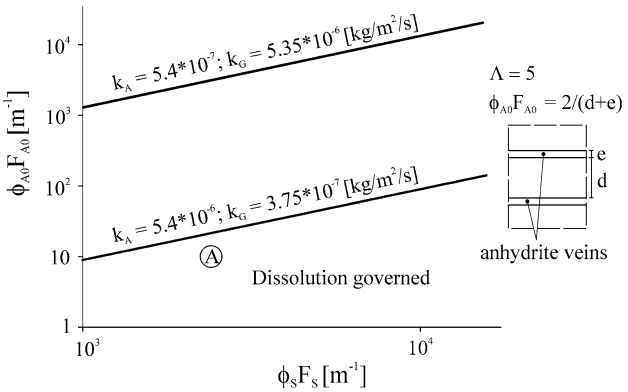

Fig. 8 Surface area of anhydrite over surface area available for gypsum growth per unit volume of the rock

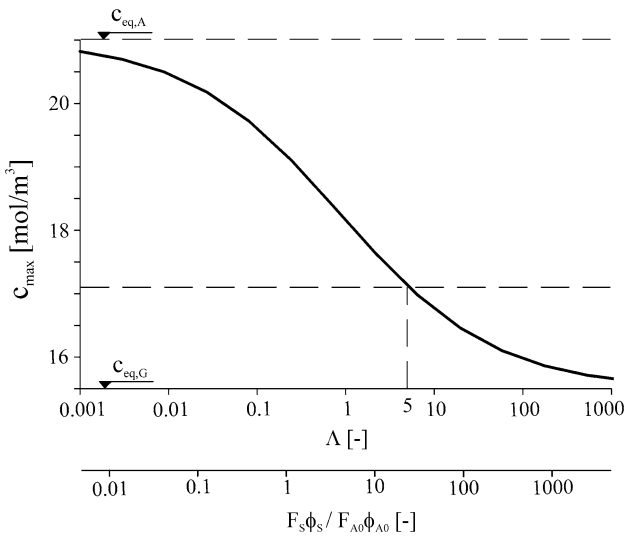

Fig. 7 Maximum concentration c_{max} over dimensionless parameter Λ

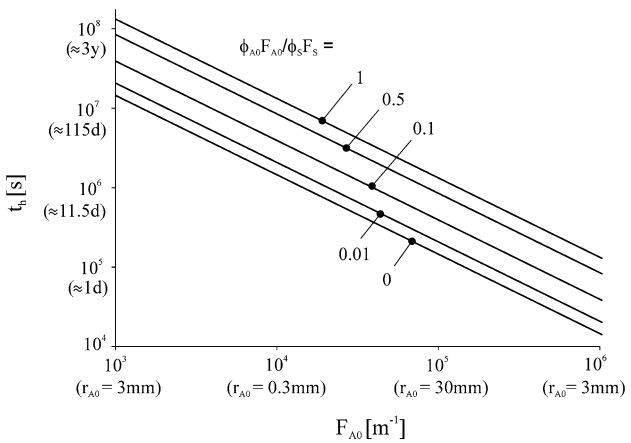

Fig. 9 Hydration time t_h over initial specific surface area of anhydrite

to the diffusion equation (Eq. 12) for different porosities n_G and thicknesses s_G of the gypsum layer. The tortuosity and the diffusion coefficient of sulphate ions through the gypsum layer (Table 1) were taken from Böhm et al. (1998) and Li and Gregory (1974), respectively. Li and Gregory (1974) give a range of $6 \div 10 \times 10^{-10}$ m^2/s for the diffusion coefficient at 20 °C.

The behaviour of the model can be explained by considering the example of a 2 mm thick gypsum layer with 10 % porosity (line 2 of Fig. 10). For concentrations to the right of the intersection of line 2 with curve 5 (point A), dissolution (curve 5) is the slowest mechanism and therefore governs the process. The transition from one mechanism to the other occurs when the two rates become equal (point A). For lower concentrations (to the left of point A), diffusion through the gypsum layer limits the dissolution rate (line 2).

Although it is not possible to estimate the porosity n_G without considering chemo-mechanical coupling, the importance of porosity becomes clear when comparing line 1 with line 4. The two lines apply to a 5 mm thick gypsum layer which has a porosity n_G of 0.5 or 0.01. The dense gypsum layer controls dissolution over practically the entire concentration range (line 4).

At the beginning of the dissolution process, the gypsum layer is still thin and its porosity is probably high, so that diffusion is not relevant in relation to the kinetics of anhydrite dissolution. With time the gypsum thickness s_G increases. The result is that the diffusion rate decreases and becomes the governing mechanism particularly in the region of low supersaturation, i.e. at concentrations close to the equilibrium concentration of gypsum $c_{eq,G}$ which are characteristic for dissolution-controlled hydration (Sect. 2.3).

Figure 11a shows how the hydration of an anhydrite layer that is initially 100 mm thick proceeds over time, assuming that gypsum crystals grow only on anhydrite and form a layer of thickness s_G. The two solid curves show the location of the gypsum–anhydrite interface (curve "$S_A/2$") and of the gypsum surface (curve "$S_{G,A}/2$") according to the standard second-order anhydrite dissolution and gypsum precipitation equations, i.e. disregarding the sealing effect of the gypsum layer on anhydrite dissolution. The distance of the two curves corresponds to the thickness s_G of the gypsum layer. It can be seen that the anhydrite core shrinks, but the total layer thickness increases by about 60 % due to the higher molar volume of gypsum.

The dashed curves incorporate the effect of sealing, i.e. they assume that the retreat rate of the dissolution front is given by Eq. (14), if this equation yields a lower value than

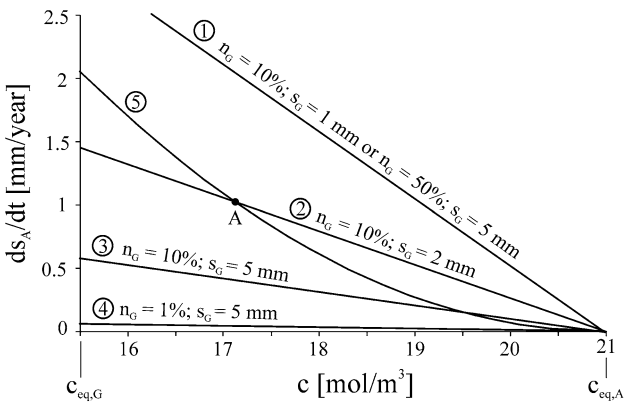

Fig. 10 Retreat rate of the anhydrite dissolution front over concentration according to the second-order reaction kinetics (*curve 5*) and the diffusion equation (lines *1–4*)

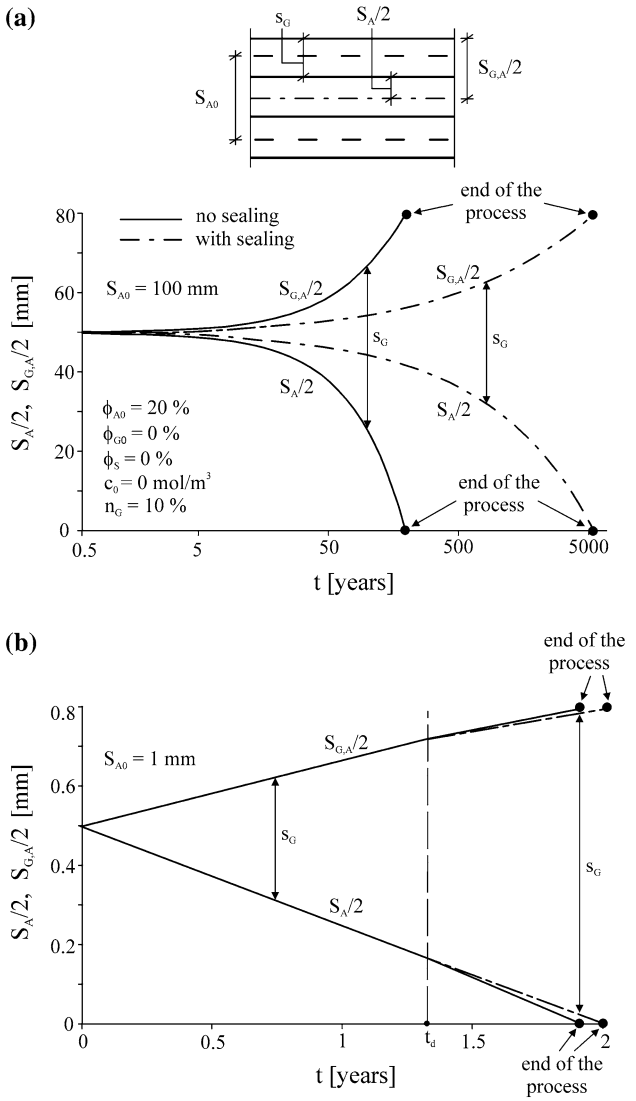

Fig. 11 Thickness of anhydrite and gypsum layer over time t **a** for a $S_{A0} = 100$ mm thick anhydrite layer and **b** for a $S_{A0} = 1$ mm thick layer with sealing taken into account (*dashed lines*) and not taken into account (*solid curves*)

Eq. (12). It can be seen that sealing delays hydration by more than one order of magnitude. This result is true only for thick anhydrite layers. Figure 11b is obtained for a 1-mm thick anhydrite vein and shows that sealing is irrelevant for this particular case. For thick anhydrite layers, sealing plays a prominent role, because only a very small percentage of the anhydrite will have hydrated by the time the gypsum thickness reaches the critical value above which diffusion retards dissolution. This actually happens so rapidly that diffusion can be regarded as the governing mechanism for almost the entire hydration process. On the other hand, for finely distributed anhydrite (Fig. 11b), most of the anhydrite will already have dissolved before the gypsum layer reaches the critical thickness (time t_d). Therefore, the effect of sealing is almost negligible.

Figure 12 shows the reduction of the volume fraction of layered anhydrite over time, for different gypsum porosities n_G and anhydrite layer thicknesses S_{A0}, assuming that gypsum growth takes place both on the anhydrite layers and on other spherical particles of inert minerals. The initial volume fractions of anhydrite and inert minerals are $\phi_{A0} = 0.2$ and $\phi_S = 0.5$, respectively. Under these conditions, the quantity of water available is sufficient for hydration of the entire quantity of anhydrite (cf. Eq. 36). Lines 3–6 apply to a 100-mm thick anhydrite layer. Line 3 disregards the effect of sealing, while lines 4–6 take into account sealing and apply to layer porosities of 0.5, 0.1 and 0.01, respectively. In the absence of sealing, the total hydration of anhydrite would take approximately 38 years. Sealing increases the hydration time to 57 years if the gypsum layer has a porosity of $n_G = 0.5$, and to 147 years for a porosity of $n_G = 0.1$. At lower porosities, hydration would be practically irrelevant for tunnelling because it would take several centuries.

Line 1 in Fig. 12 corresponds to the case of finely distributed anhydrite ($S_{A0} = 1$ mm). For gypsum layer

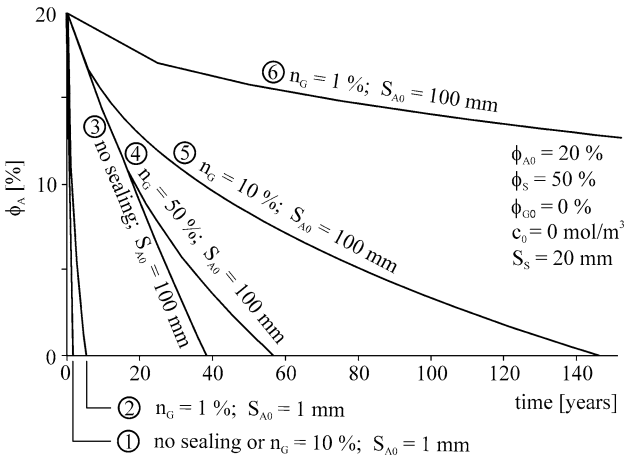

Fig. 12 Volume fraction of anhydrite over time for different anhydrite layer thicknesses and gypsum layer porosities

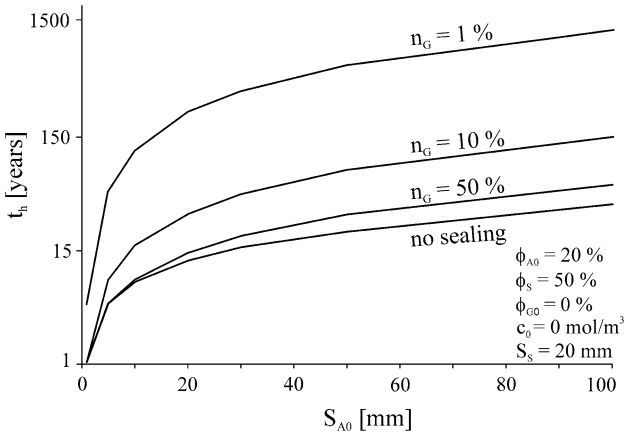

Fig. 13 Hydration time of an anhydrite layer as a function of its initial thickness

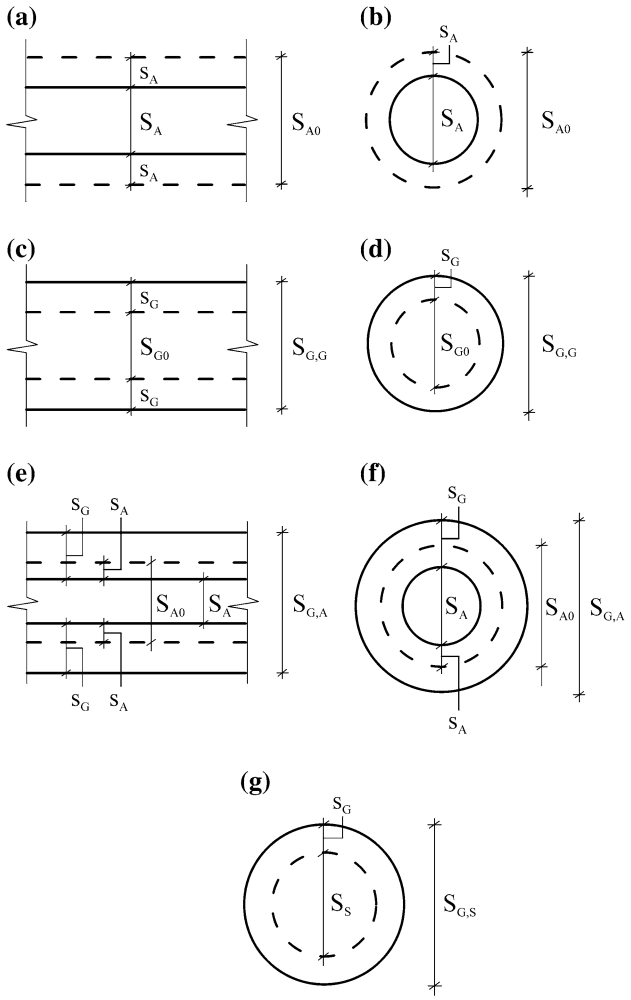

Fig. 14 **a**, **b** Anhydrite particles during dissolution; **c**, **d** gypsum particles during precipitation; **e**, **f** anhydrite particles sealed by a gypsum layer **g** inert solid particle with precipitated gypsum

porosities n_G of 0.1 or more, sealing does not affect the hydration duration. However, for a very low porosity ($n_G = 0.01$, line 2), the hydration time amounts to more than 5 years, i.e. three times more than without sealing (line 1). To summarise, sealing is important for thick anhydrite layers. In the case of finely distributed anhydrite, sealing plays a role only if the formed gypsum is very dense.

Finally, Fig. 13 shows the total hydration time t_h as a function of the initial anhydrite layer thickness for different gypsum porosities n_G, with and without the anhydrite sealing being taken into account. Figure 13 makes clear once more the importance of gypsum porosity and particle size in terms of the sealing effect and thus the time evolution of the hydration process.

The modelling results agree with (and provide an explanation for) the general observation made in tunnelling that thicker anhydrite veins and layers do not swell (cf. Sect. 2.4).

6 Conclusions

A model has been developed and calibrated with existing experimental results for the simultaneous dissolution of anhydrite and precipitation of gypsum in a closed system, taking into account the sealing effect caused by the precipitation of gypsum on the anhydrite mineral. After performing parametric studies for the case of simultaneous anhydrite dissolution and gypsum precipitation omitting the sealing effect, a simple relationship has been proposed in order for the anhydrite dissolution to represent the limiting mechanism. The investigations have shown that this is the case when anhydrite takes the form of veins with a thickness of 1 mm, for example, and when gypsum precipitation takes place on spherical particles of inert minerals with a radius of 0.1 mm. It has also been shown that the time required for the whole amount of anhydrite to hydrate may vary by orders of magnitude. Moreover, for systems where dissolution is the governing mechanism, the initial volume fraction of anhydrite does not play any role in terms of the hydration time.

The effect of sealing has been shown to be decisive for the time evolution of the hydration process where gypsum with low porosity precipitates on thick layers of anhydrite. Depending on the gypsum porosity and the thickness of the anhydrite layers, the hydration time of anhydrite may increase by many orders of magnitude and exceed by far the usual service life of tunnels (100 years). The quantitative results explain theoretically the well-known observation that anhydrite layers of at least a few centimetres thick hardly swell at all.

It should be kept in mind that the investigations were performed with the assumption that a sufficient quantity of water was available. However, this is not always the case in nature, as the flow of water to the anhydrite surface may be hindered either by pores becoming clogged due to the precipitation of gypsum, or by the existence of a clay matrix which tends to absorb water. Consequently, the actual hydration times may be considerably higher. Transport processes and interaction of anhydrite with the clay matrix are probably important in this respect.

7 Appendix

The volume fraction of anhydrite

$$\phi_A = \frac{\phi_{A0}}{a_A b_A} \bar{S}_A (\bar{S}_A + a_A - 1)(\bar{S}_A + b_A - 1) \tag{A1}$$

in the case of parallelepipeds (Fig. 14a), while for spherical particles (Fig. 14b)

$$\phi_A = \phi_{A0} \bar{S}_A^3, \tag{A2}$$

where

$$\bar{S}_A = S_A / S_{A0} = 1 + 2\bar{s}_A. \tag{A3}$$

In the case of parallelepipedic gypsum particles (Fig. 14c),

$$\phi_{G,G} = \phi_{G0} \left(\frac{\bar{S}_{G,G}(\bar{S}_{G,G} + a_G - 1)(\bar{S}_{G,G} + b_G - 1)}{a_G b_G} - 1 \right) \times (1 - n_G), \tag{A4}$$

while for spherical gypsum particles (Fig. 14d):

$$\phi_{G,G} = \phi_{G0} \left(\bar{S}_{G,G}^3 - 1 \right)(1 - n_G), \tag{A5}$$

where

$$\bar{S}_{G,G} = S_{G,G} / S_{G0} = 1 + 2\bar{s}_G. \tag{A6}$$

The volume fraction $\phi_{G,A}$ of the gypsum growing on parallelepipedic or spherical anhydrite particles (Fig. 14e, f) is given by the following equations:

$$\phi_{G,A} = \frac{\phi_{A0}}{a_A b_A} \left[\bar{S}_{G,A}(\bar{S}_{G.A} + a_A - 1)(\bar{S}_{G,A} + b_A - 1) - \bar{S}_A(\bar{S}_A + a_A - 1)(\bar{S}_A + b_A - 1) \right](1 - n_G), \tag{A7}$$

$$\phi_{G,A} = \phi_{A0} \left[\bar{S}_{G,A}^3 - \bar{S}_A^3 \right](1 - n_G). \tag{A8}$$

where

$$\bar{S}_{G,A} = S_{G,A} / S_{A0} = \bar{S}_A + 2\bar{s}_G. \tag{A9}$$

Finally, the volume fraction of gypsum $\phi_{G,S}$ formed on inert solids of spherical shape (Fig. 14g) is equal to:

$$\phi_{G,S} = \phi_S\left(\bar{S}_{G,S}^3 - 1\right)(1 - n_G), \tag{A10}$$

where

$$\bar{S}_{G,S} = S_{G,S}/S_{A0} = \bar{S}_S + 2\bar{s}_G \tag{A11}$$

and

$$\bar{S}_S = S_S/S_{A0}. \tag{A12}$$

Acknowledgments This paper evolved within the framework of the research project 'Modelling of anhydritic swelling claystones' which is being carried out at the ETH Zurich, being financed by the Swiss National Science Foundation (SNF) and the Swiss Federal Roads Office (FEDRO).

References

Amstad C, Kovári K (2001) Untertagbau in quellfähigem Fels. Schlussbericht Forschungsauftrag 52/94 des Bundesamts für Strassen ASTRA

Anagnostou G, Pimentel E, Serafeimidis K (2010) Swelling of sulphatic claystones—some fundamental questions and their practical relevance. Geomech Tunn 3 (5):567–572

Anderson GM (1996) Thermodynamics of natural systems. John Wiley and Sons, Inc., University of Toronto

Andreae C (1956). Gebirgsdruck und Tunnelbau. Schweizerische Bauzeitung 74:107–110

Appelo CAJ, Postma D (2005) Geochemistry, groundwater and pollution, 2nd edn. A. A. Balkema, Rotterdam

Atkins P, de Paula J (2006) Atkins'Physical Chemistry, 8th edn. Oxford University Press, Oxford

Bezjak A, Jelenic I (1980) On the determination of rate constants for hydration processes in cement pastes. Cem Concr Res 10:553–563

Bishnoi S (2008) Vector modelling of hydrating cement microstructure and kinetics. Dissertation No 4093, École Polytechnique Fèdèrale de Lausanne

Bishnoi S, Scrivener LK (2009) Studying nucleation and growth kinetics of alite hydration using μic. Cem Concr Res 29:849–860

Böhm M, Devinny J, Jahani F, Rosen G (1998) On a moving-boundary system modeling corrosion in sewer pipes. Appl Math Comput 92:247–269

Böhringer J, Jenni JP, Hürlimann P, Resele G, Grauer R, Norbert J (1990) Anhydritvorkommen als Wirtgestein für die Lagerung schwach- und mittelaktiver Abfälle dargestellt am Beispiel des Bois de la Glaive. NAGRA, Technischer Bericht, pp 88–15

Brantley SL, Kubicki JD, White AF (2008) Kinetics of water–rock interaction. Springer, New York

Einstein HH (1996) Tunnelling in difficult ground—swelling behaviour and identification of swelling rocks. Rock Mech and Rock Eng 29(3):113–124

Freyer D, Voigt W (2003) Crystallization and phase stability of $CaSO_4$—based salts. Monatsh Chem 134:693–719

Gassmann J, Gysel M, Schneider JF (1979) Anhydrit als Wirtgestein für die Endlagerung radioaktiver Abfälle in der Schweiz. Technical Report Nagra, No. 12, Baden

Grob H (1972) Schwelldruck im Belchentunnel. Internationales Symposium für Untertagbau, Luzern, pp 99–119

Henke KF, Kaiser W (1975) Zusammenfassung und Deutung der Ergeb-nisse in Bezug auf Sohlhebungen beim Tunnelbau im Gipskeuper. Durch-führung eines felsmechanischen Grossversuches in der Nordröhre des Wagenburgtunnels in Stuttgart. Schriftenhefte Strassenbau und Strassen-verkehrs-tech-nik 184:185–195

Henke KF, Kaiser W, Nagel D (1975) Geomechanische Untersuchungen im Gips-keuper. Durchführung eines felsmechanischen Grossversuches in der Nord-röhre des Wagenburgtunnels in Stuttgart. Schriftenhefte Strassenbau und Strassen-verkehrs-technik 184:149–162

Kontrec J, Kralj D, Brečević L (2002) Transformation of anhydrous calcium sulphate into calcium sulphate dihydrate in aqueous solutions. J Cryst Growth 240:203–211

Langbein R, Peter H, Schwahn H (1982) Karbonat und Sulfatgesteine. Deutscher Verlag für Grundstoffindustrie, Leipzig

Lasaga CA (1986) Metamorphic reaction rate laws and development of isograds. Miner Mag 50:359–373

Lasaga CA (1998) Kinetic theory in earth sciences. Princeton University Press, NJ

Lasaga CA, Rye DM (1993) Fluid flow and chemical reaction kinetics in metamorphic systems. Am J Sci 293:361–404

Li YH, Gregory S (1974) Diffusion of ions in sea water and in deep-sea sediments. Geochim Cosmochim Acta 38:703–714

Madsen FT, Nüesch R (1990) Langzeitverhalten von Tongesteinen und tonigen Sulfatgesteinen. Mitteilungen des Institutes für Grundbau und Bodenmechanik, Eidgenössische Technische Hochschule Zürich, Nr.140

Müller WH, Briegel U (1977) Experimentelle Untersuchungen an Anhydrit. Bericht Nr. 2. Geol. Institut der ETH Zürich, Arbeitsgruppe Anhydrite der Nagra

Mullin JW (2001) Crystallization, 4th edn, Butterworth-Heinemann, Oxford

Nancollas GH, Purdie N (1964) The kinetics of crystal growth. Q Rev Chem Soc 18:1–20

Pignat C, Navi P, Scrivener K (2005) Simulation of cement paste microstructure hydration pore space characterization and permeability determination. Mater Struct 38:459–466

Sahores J (1962) Contribution à l' ètude des phènomenes mèchaniques accompagnant l' hydratation de l' anhydrite. Dissertation, Revue des matèriaux de construction

Serafeimidis K, Anagnostou G (2012a) On the kinetics of the chemical reactions underlying the swelling of anhydritic rocks. Eurock 2012, Stockholm

Serafeimidis K, Anagnostou G (2012b) Simultaneous anhydrite dissolution and gypsum precipitation in a closed swelling rock system. ARMA 2012, Chicago

Steefel CI, Lasaga CA (1994) A coupled model for transport of multiple chemical species and kinetic precipitation/dissolution reactions with application to reactive flow in single phase hydrothermal systems. Am J Sci 294:529–592

Steefel CI, Van Cappellen P (1990) A new kinetic approach to modeling water-rock interaction: the role of nucleation, precursors and Ostwald ripening. Geochemica et Cosmochimica 54:2657–2677

Wiesmann E (1914) Über die Stabilität von Tunnelmauwerk unter Berücksichtigung der Erfahrungen beim Bau des Hauenstein-Basistunnel. Schweizerische Bauzeitung 64(3):27–32